

A graph neural network-based model with Out-of-Distribution Robustness for enhancing Antiretroviral Therapy Outcome Prediction for HIV-1

Giulia Di Teodoro^{a,b,**}, Federico Siciliano^{a,*}, Valerio Guarrasi^{c,*},
Anne-Mieke Vandamme^{e,f}, Valeria Ghisetti^g, Anders Sönnnerborg^{h,i},
Maurizio Zazzi^d, Fabrizio Silvestri^a, Laura Palagi^a

^a*Sapienza University of Rome, Department of Computer Control and Management
Engineering Antonio Ruberti, 00185, Rome, Italy*

^b*EuResist Network, 00152, Rome, Italy*

^c*Unit of Computer Systems and Bioinformatics, Department of Engineering, University
Campus Bio-Medico of Rome, 00128, Rome, Italy*

^d*Department of Medical Biotechnologies, University of Siena, 53100, Siena, Italy*

^e*KU Leuven, Department of Microbiology, Immunology and Transplantation, Rega
Institute for Medical Research, Clinical and Epidemiological Virology, Leuven, Belgium*

^f*Center for Global Health and Tropical Medicine, Instituto de Higiene e Medicina
Tropical, Universidade Nova de Lisboa, 1349-008, Lisbon, Portugal*

^g*Molecular Biology and Microbiology Unit, Amedeo di Savoia Hospital, ASL Città di
Torino, 10128, Turin, Italy*

^h*Karolinska Institutet, Division of Infectious Diseases, Department of Medicine
Huddinge, 14152, Stockholm, Sweden*

ⁱ*Karolinska University Hospital, Department of Infectious
Diseases, 14186, Stockholm, Sweden*

Abstract

Predicting the outcome of antiretroviral therapies for HIV-1 is a pressing clinical challenge, especially when the treatment regimen includes drugs for which limited effectiveness data is available. This scarcity of data can arise either due to the introduction of a new drug to the market or due to limited use in clinical settings. To tackle this issue, we introduce a novel joint fusion

*These authors contributed equally to the paper

**Corresponding author. email: diteodoro@diag.uniroma1.it

model, which combines features from a Fully Connected (FC) Neural Network and a Graph Neural Network (GNN). The FC network employs tabular data with a feature vector made up of viral mutations identified in the most recent genotypic resistance test, along with the drugs used in therapy. Conversely, the GNN leverages knowledge derived from Stanford drug-resistance mutation tables, which serve as benchmark references for deducing in-vivo treatment efficacy based on the viral genetic sequence, to build informative graphs. We evaluated these models' robustness against Out-of-Distribution drugs in the test set, with a specific focus on the GNN's role in handling such scenarios. Our comprehensive analysis demonstrates that the proposed model consistently outperforms the FC model, especially when considering Out-of-Distribution drugs. These results underscore the advantage of integrating Stanford scores in the model, thereby enhancing its generalizability and robustness, but also extending its utility in real-world applications with limited data availability. This research highlights the potential of our approach to inform antiretroviral therapy outcome prediction and contribute to more informed clinical decisions.

Keywords: Human Immunodeficiency Virus; Out-of-distribution; Graph Neural Network; therapy prediction; Stanford score.

1. Introduction

Human immunodeficiency virus (HIV) is an infectious agent that attacks the immune system, and if not treated properly, it can lead to severe consequences. It was discovered in 1981 and thereafter it has infected more than 80 million people and caused the deaths of more than 40 million. By the end

of 2021, the World Health Organization estimated that, globally, about 38.4 million people were living with HIV [1]. There are no vaccines for HIV, and it cannot be cured yet. Despite this, with regular treatment and high-quality health care, people living with HIV (PLHIV) can have a life expectancy comparable to that of people not infected by the virus.

Antiretroviral therapy (ART) has been shown to be effective in controlling viral replication for most PLHIV. If no ART is used, HIV-infected patients come to manifest symptoms of acquired immunodeficiency syndrome (AIDS). Commonly, an ART usually consists of a cocktail of three antiretroviral drugs that cooperatively block virus replication at multiple steps and, compared to a single drug, are successful in prolonging the time it takes for HIV to become resistant to therapy. This success is due to the development of potent and well-tolerated antiretroviral drugs with high genetic barriers to resistance. As a result, it is increasingly common to switch patients under prolonged successful therapy to a simplified and highly tolerated regimen, even a dual-drug regimen. However, before a change of therapy, patient records should be carefully analyzed to guide treatment choices and preserve future treatment options. This includes reviewing past drug exposure, treatment failures, cumulative drug resistance, and duration of virological suppression [2, 3].

By examining the correlation between HIV-1 mutational patterns and drug resistance, it is possible to interpret a genotype and provide a model of drug susceptibility. There are two types of genotype interpretation systems: rule-based systems and systems based on statistical or Machine Learning (ML) models. The former use tables of drug resistance mutations, created and maintained by experts, to generate a drug resistance score that classifies

the genotype in several drug susceptibility categories that go from being full susceptible to completely resistant [4, 5, 6]. The latter is trained directly on genotypic data for predicting therapy outcomes [7, 8, 9].

With the availability of increasing amounts of genotypic and clinical data, ML models have become widely used to guide treatment choices, especially for treatment-experienced patients with complicated drug-resistance profiles. However, when training ML models to predict treatment outcomes, it is possible that some treatment regimens may be excluded from the training set because there is not wide availability of data regarding one or more drugs specifically. This could happen when the drug in question is rarely used in drug regimens or has been launched on the market too recently and, consequently, data on the efficacy of therapies containing it are missing or not yet accessible. In this scenario, classical ML models cannot be used to predict the outcome of drug regimens containing drugs not included in the model’s training set. At the same time, rule-based systems may be inaccurate when assigning a susceptibility score to a therapy containing a new drug because of limited clinical experience with that drug. In fact, when regulatory agencies approve a new drug, drug resistance scores related to mutations are mainly created based on in-vitro experiments with validation of resistance contribution by site-directed mutagenesis and susceptibility testing of laboratory or clinical isolates [4]. It may be the case that the clinical trial enrolled only patients without mutations, on first-line therapy, so there is not yet a relationship between mutations and drug efficacy in-vivo. Therefore, the created scores are preliminary and may be subject to later adjustment.

To fill this gap, we propose a model using Graph Neural Networks (GNNs)

[10] which are able to incorporate knowledge derived from the drug-resistance mutation tables [11]. In this way, we can accurately predict the outcome of therapies that contain drugs for which no data were present in the training phase but are present in the knowledge base.

In the following, in section 2 we describe the state-of-the-art of HIV genotypic interpretation systems and present an overview of techniques used to solve the Out of Distribution problem and how GNNs function and how they could be useful in this context. In section 3 we present the data used by the methodology presented in section 4. Next, in section 5 we present the different experiments implemented to obtain the results presented and discussed in section 6. Finally, in section 7 we conclude by highlighting the main findings opening future work for the following research.

2. Related Work

2.1. HIV Genotypic Interpretation Systems

Antiretroviral treatments against HIV-1 can lead to the emergence of mutations in the virus that make it drug-resistant. These variants can become predominant under drug pressure and cause treatment failure. Thus, testing for resistance has become an integral part of the clinical management of PL-HIV. Two main methods for studying HIV-1 resistance to antiretroviral drugs are genotypic resistance tests (GRTs) and in-vitro phenotypic tests [12]. The former detects resistance mutations and infers drug activity based on known correlations between drug mutations and response to therapy in-vivo, while the latter measures the concentration of the replication-inhibiting drug in standardized but complex virus-cell systems in-vitro. Genotypic resistance

tests are commonly used in clinical practice since phenotypic tests are not amenable to clinical practice.

Genotypic drug resistance interpretation systems (GIS) can be classified into two main types: rule-driven and data-driven methods.

Rule-based systems use tables formulated by experts that indicate which mutations cause resistance to certain types of drugs [11]. These tables guide the assignment of resistance scores to specific genotypes. The main rule sets from ANRS, HIVdb [13], HIV-GRADE and Rega Institute are accessible on the HIV-GRADE [14] platform. Drug resistance scores and consequently rule-based approaches are updated frequently to reflect new findings on HIV drug resistance based on expert consensus [15]. They often rely on data from Sanger sequencing, an established technique prized for its accuracy and cost-effectiveness. However, low-frequency resistant variants [16][17], which may be clinically significant [18][19], may not be detected by Sanger sequencing. Instead, next-generation sequencing (NGS) methods [20] can identify resistant strains that constitute as little as 1% of the viral population, compared with about 20% by Sanger sequencing. NGS methods are increasingly being used. These NGS results are usually processed using the same interpretation systems as Sanger sequencing data, although the clinical implications of low-frequency resistance remain an ongoing topic of discussion.

In contrast, data-driven GISs exploit statistical or ML algorithms to interpret resistance from the data directly. Given the large volume of clinical and genotypic data available, data-driven systems have become vital for clinicians, particularly in treating patients with complicated drug resistance profiles developed over time. Early iterations of data-driven GIS, such as Virco-

TYPE’s VirtualPhenotypeTM [21] and the geno2pheno framework [22], aimed to predict the phenotype *in-vitro*. VircoTYPE initially calculated the phenotypic effect by pooling the impacts of individual mutations on individual drugs via a linear regression algorithm, later modified to provide clinically actionable resistance estimates [23]. Geno2pheno, on the other hand, originally served to estimate single-drug resistance and was later extended to predict 3-4-drug ART outcomes. Geno2pheno-THEO used both genotypic information and user-provided data to predict the probability of treatment success [24]. Geno2pheno[resistance][25][26] makes use of a support vector machine model to estimate specific drug resistance, while Geno2pheno[drug exposure][27] first calculates drug exposure scores and then uses these scores in a second model used for predicting treatment outcome. Other platforms, such as SHIVA, use random forests for similar purposes [28], and one study even used artificial neural networks for this purpose [29].

2.2. Out of Distribution

The concept of Out of Distribution (OoD) has garnered significant attention in various fields due to its implications for ML, pattern recognition, and classification tasks. OoD refers to scenarios in which a model encounters data samples that significantly differ from the distribution it was trained on, leading to potential performance degradation or erroneous predictions.

In a foundational work, Hendrycks & Gimpel [30] proposes a baseline method for OoD detection by using a simple threshold on predictive uncertainty. They introduce metrics such as Maximum Softmax Probability to identify misclassified and OoD samples. In [31], Liang et al. build upon the previous work [30], presenting a method that calibrates the uncertainty esti-

mates of neural networks using temperature scaling to improve OoD detection accuracy. Addressing the limitations of single-model uncertainty estimation, Lakshminarayanan et al. [32] propose the use of deep ensembles to enhance OoD detection. The authors showcase that by averaging predictions of multiple models, more accurate uncertainty estimates can be obtained, leading to improved OoD classification. The field of OoD detection has witnessed significant growth in recent years, with researchers proposing diverse approaches to enhance the reliability of models when facing novel and unexpected data samples. The referenced papers highlight key milestones, methodologies, and datasets that have contributed to the advancement of OoD detection techniques, enabling more robust and reliable ML systems.

In the context of medical applications, the need for reliable and accurate predictions is paramount. OoD detection techniques play a crucial role in ensuring the safety and effectiveness of ML models when dealing with novel and unexpected data samples. In [33], the authors address the challenge of selecting appropriate OoD detection methods for medical imaging tasks. The study highlights the importance of distinguishing between various categories of OoD examples and showcases the limitations of existing methods in recognizing images that are close to the training distribution. Next, in [34] introduces the Medical-OoD-Analysis-Challenge as a comprehensive benchmark for evaluating OoD detection methods in the medical imaging domain. With a focus on the importance of reliable predictions in medical applications, the challenge evaluates algorithms' performance in detecting deviations from the training distribution. Finally, [35] addresses the practical challenges of implementing OoD detection methods in the context of

medical applications, particularly Electronic Health Records. The authors provide a set of guidelines and tests to aid in the selection of suitable OoD detectors for specific medical datasets.

While the concept of OoD detection and mitigation has gained substantial attention across the medical domain, it appears that there is a notable absence of specific research addressing OoD challenges within the context of HIV treatment response prediction. Our research addresses this existing gap in the application of OoD concepts to HIV prediction. Moreover, our research aims to diverge from the conventional approach of solely focusing on OoD detection: rather than identifying and flagging OoD instances, our focus is to cultivate model robustness against OoD scenarios in the realm of HIV therapy prediction. Our efforts contribute to the development of more reliable and effective predictive models for HIV prognosis, ultimately leading to improved patient care and treatment decision-making.

2.3. Graph Neural Networks

In the world of data, not all structures are created equal. While conventional neural networks have achieved impressive results for grid-like data structures (e.g., images and sequences), many real-world problems involve more intricate, non-Euclidean data forms. Here is where graphs, which can model a wide range of complex systems, from molecular structures to social networks, come into play.

A graph G is defined by a set of nodes V and a set of edges E , where an edge represents a relationship between two nodes. In many applications, nodes and/or edges have attributes or features associated with them. Integrating graph theory with deep learning led to the birth of GNNs [36]. The

central idea behind GNNs is to update the representation of a node by aggregating information from its neighbors. This aggregation procedure captures the local structure of the graph and can be iteratively applied to capture information from further away in the graph. A typical GNN layer involves several interconnected stages. First, for each node, feature information from its neighbors is aggregated. This aggregation can range from a simple mean of the neighbor features to more intricate operations. Following aggregation, this gathered information is combined with the node’s current feature. Lastly, to transform the combined feature, a neural network layer, often a fully connected one, is applied. This GNN layer operation can be described as:

$$h_i^{(l+1)} = \sigma \left(W^{(l)} \cdot \text{COMBINE} \left(h_i^{(l)}, \text{AGGREGATE} \left(\{h_j^{(l)} : j \in \text{Neighbors}(i)\} \right) \right) \right) \quad (1)$$

Where $h_i^{(l)}$ is the feature of node i at layer l , $W^{(l)}$ is the weight matrix for layer l , and σ is a non-linear activation function.

GNNs may be used for different tasks, e.g., graph classification, node classification and link prediction.

Several variants of GNNs have been proposed, with different aggregation and combination functions, of which Graph Convolutional Networks (GCN) [37] have proven state-of-the-art results in the biomedical field [38]. Inspired by the successes of CNNs on grid-structured data, the GCN attempts to generalize convolutional operations to irregular graph structures. In a GCN, each node gathers information from its direct neighbors. The updated feature for a node is typically a combination of its own features and the average (or another form of aggregation) of its neighbors’ features.

This process can be thought of as a form of weighted averaging, where the weights often come from the edge information or are learnable parameters. The operation for a layer in a GCN can be given as:

$$h_i^{(l+1)} = \sigma \left(W^{(l)} \cdot \text{MEAN} \left(\{h_i^{(l)}\} \cup \{h_j^{(l)} : j \in \text{Neighbors}(i)\} \right) \right) \quad (2)$$

Where $h_i^{(l)}$ represents the feature vector of node i at the l -th layer, $W^{(l)}$ is a learnable weight matrix for the l -th layer, and σ denotes a non-linear activation function.

GNNs have found significant applications in the realm of biomedicine [38]. In drug discovery and molecular chemistry, molecules are represented as graphs where atoms form the nodes and bonds act as edges [39]. Through this representation, GNNs have been pivotal in predicting molecular properties and activities, thus streamlining drug design and discovery processes. Additionally, they play a role in anticipating compound-protein interactions, which is essential for drug repurposing. In the domain of protein structure and functionality, GNNs analyze protein-protein interaction networks to predict protein functions or discern unknown interactions [40]. They also offer insights into the complex task of protein folding by viewing amino acids as nodes and their interactions as edges to determine protein 3D structures. Genomics and genetics benefit from GNNs by utilizing them to model and infer interactions in gene regulatory networks [41]. Moreover, they assist in discerning the functional consequences of genetic variations by capturing the relational structures between genomic regions. In medical imaging, GNNs have shown their prowess in tasks such as tumor segmentation or organ recognition by modeling connections between various regions of interest in the images [42]. In the context of electronic health records, GNNs en-

hance our understanding by examining similarities between patients based on factors like diagnosis or treatment history, helping predict disease progression or treatment outcomes [43]. In the realm of neuroscience, GNNs are instrumental in analyzing brain connectivity data to probe into disorders or understand the functional organization of the neural landscape [44].

GNNs in the context of HIV research have potential applications primarily in drug discovery [45] and molecular chemistry [46]. Given the complex nature of HIV and its propensity to mutate, understanding the molecular structures and interactions of the virus and potential drugs is critical. By representing the HIV proteins or potential anti-HIV compounds as graphs, GNNs can be utilized to predict molecular properties, activities, and interactions that might be effective against the virus. To the best of our knowledge, there is a lack of literature on using GNN for OoD in the HIV framework. In this context, GNN-based models have been used mainly to learn molecule representation, such as in [47] where a geometric deep learning approach is used to rapidly and inexpensively assess the pharmacological potential of molecules by predicting HIV drug resistance and virus-drug interaction. Also, in [48], the DeepAAI method is proposed. It generates a new way to represent HIV antibodies by building two dynamic relational graphs that connect antibodies and antigens and using Laplacian smoothing to harmonize the features of both known and previously unobserved antibodies. Finally, in [49], a graph neural network-based molecular feature extraction model has been proposed to improve the prediction of potential multiple targets of HIV-1 and HBV simultaneously.

3. Dataset

The Euresist Integrated Database (EIDB) [50] is one of the largest databases containing data on PLHIV, both treatment-naïve and treatment-experienced, who have been followed since 1998. Established in 2006, the EIDB collects information from nine national cohorts: Italy, Germany, Sweden, Portugal, Spain, Luxembourg, Belgium, Turkey, and Russia. It has recently been expanded with data from Ukraine and Georgia. The data, in anonymized form, cover demographic and clinical aspects of PLHIV, such as types of antiretroviral therapies, reasons for therapy changes, treatment responses, CD4+ cell counts, viral load (VL) measurements, AIDS defining events, and additional viral co-infections. The database includes data from 105101 PLHIV, but the information from many patients is not consistent enough for our analysis. The database has been analyzed to select consistent and complete data to be part of the dataset used in the experiments of the paper.

The model we propose is therapy-oriented and therefore the data are structured according to therapy-patient pairs. In the analysis of treatment success or failure, the concepts of the patient-treatment episode (PTE) is delineated, as mentioned in previous research [51].

Definition PTE. *This episode is a collection of data for a patient to assess the response to a treatment. It consists of a genotype (protease (PR) reverse transcriptase (RT) and/or integrase (IN)) at baseline, the group of pharmacological compounds used in antiretroviral treatment (cART), an optional VL at baseline, taken no more than 90 days before the start of treatment, and follow-up VLs. PTEs include both first-line therapy and treatment change episodes referred to a patient.*

The dataset we built contains information coming from PTEs. The outcome of drug treatment is indicated with a label, $y \in \{0, 1\}$, representing success or failure. This is based on a recently adopted definition of the Eu-Resist standard datum.

Definition Standard datum. *To determine the success of a therapy, a follow-up VL, and optionally a VL at the baseline, is needed. All the follow-up VLs measured between 20 and 28 weeks after therapy initiations are taken. Among them, the VL whose measurement day is closer to the 24th week is considered. The PTE is labeled as a success if this follow-up VL is less than 50 copies of HIV-1 RNA per milliliter of blood plasma. Alternatively, the treatment for that patient is considered a failure.*

For cases where treatment was modified before reaching the 24-week, the following criteria are used:

- *Therapies that last 4 weeks at maximum are not included because they are most likely terminated due to adverse effects.*
- *Therapies that last from 4 to 8 weeks are considered a success if the VL is under 50 copies/ml or shows at least 1 log reduction compared to the last detected VL; otherwise, they are considered a failure.*
- *Therapies that last from 8 to 20 weeks are considered a success if the VL is under 50 copies/ml or shows at least 2 log reduction compared to the last detected VL; otherwise, they are considered a failure.*

To be included in the dataset, a patient-therapy pair must fulfill the following requirements:

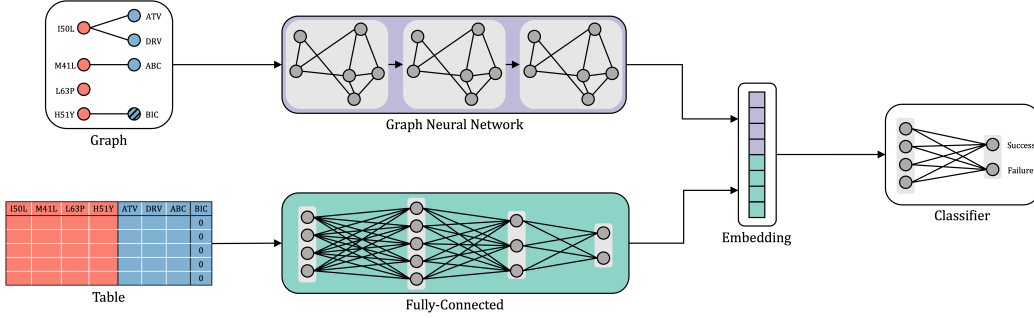
- Conform to the definition of PTE, including details of the compounds used, at least one genotypic sequence before the start of therapy and the follow-up VL.
- The success or failure of the patient’s therapy must be able to be determined in accordance with the definition of Standard Datum.

The drugs included in the dataset are listed: lamivudine (3TC), abacavir (ABC), amprenavir (APV), atazanavir (ATV), zidovudine (AZT), bicittegravir (BIC), cabotegravir (CAB), stavudine (D4T), zalcitabine (DDC), didanosine (DDI), delavirdine (DLV), doravirine (DOR), darunavir (DRV), dolutegravir (DTG), efavirenz (EFV), etravirine (ETR), elvitegravir (EVG), fosamprenavir (FPV), emtricitabine (FTC), indinavir (IDV), lopinavir (LPV), nelfinavir (NFV), nevirapine (NVP), raltegravir (RAL), rilpivirine (RPV), saquinavir (SQV), tenofovir alafenamide (TAF), tenofovir disoproxil (TDF), tipranavir (TPV).

Both polymorphic and non-polymorphic mutations are considered, with the rationale that unrecognized mutations or combinations could influence the virus’s susceptibility to cART or its fitness. Polymorphisms are mutations frequently ($\geq 1\%$) occurring in viruses not exposed to selective drug pressure. A nonpolymorphic or minimally polymorphic mutation does not occur in the absence of therapy [52].

Ultimately, the dataset consists of 22000 patient-therapy pairs: 12386 successes and 9614 failures.

Figure 1: Schematic view of the pipeline.



4. Methodology

4.1. Setting

Let's define m_j as a particular mutation, with $m_j \in M = \{m_1, m_2, \dots, m_{N_M}\}$, where M contains all the mutations considered. d_k represents an individual drug, $d_k \in D = \{d_1, d_2, \dots, d_{N_D}\}$, comprising the drugs under examination. N_M represents the total number of mutations in consideration, while N_D denotes the total number of drugs being studied.

We introduce a binary vector $r \in \{0, 1\}^{N_M}$, which flags the presence of drug-resistant mutations (DRMs) that have been observed in the last available viral genotype prior to initiating the antiretroviral treatment of interest. Additionally, $z \in \{0, 1\}^{N_D}$ is a binary vector that specifies the combination of drugs employed in the target ART for which we want to predict the outcome. A binary label $y \in \{0, 1\}$ categorizes the treatment as either successful ($y = 0$) or unsuccessful ($y = 1$), based on criteria outlined in the Standard Datum definition given in section 3. The model we propose uses the dataset both in tabular form and with data graph structures, as it

can be seen in Figure 1. Here below, it is explained how these two data types are treated.

4.2. Tabular data

The tabular data consists of a set of records in which each data point corresponds to a unique patient-treatment pair $x_i = (r_i, z_i)$, along with the associated outcome y_i . Thus, each data point can be represented as a triplet (r_i, z_i, y_i) . The training set $T = \{(r_1, z_1, y_1), \dots, (r_N, z_N, y_N)\}$ is assembled, where N is the total number of patient-treatment pairs.

4.3. Graph data

There exist a relationship $s_{m_j d_k} \in [-1, +1]$ between a mutation $m_j \in M$ and a drug $d_k \in D$. These drug-mutation relationships are shown in the Stanford tables and are regarded in HIVdb as genotypic resistance scores [13]. The score associated with a drug-mutation pair $s_{m_j d_k}$, which we will refer to as the Stanford score, is higher the more a mutation decreases the susceptibility of the virus to a drug.

For each tabular record $(x_i, y_i) = (r_i, z_i, y_i)$, we generate a graph structure, where each patient-drug sample (x_i, y_i) is represented by a graph. Nodes in the graph represent both mutations and drugs. The edges are directional and connect a mutation node n_{m_j} to a drug node n_{d_k} if a Stanford score $s_{m_j d_k}$ is associated with that mutation-drug pair; nodes not involved in any mutation-drug pair and for which a Stanford score exists remain isolated nodes. Each node, n_{d_k} or n_{m_j} , in the graph has a binary attribute r_{ij} or z_{ik} , respectively, valued at 1 if the corresponding mutation m_j or drug d_k is present in the record r_i or z_i , respectively, 0 otherwise. Each edge $e_{m_j d_k}$ in

the graph connecting a mutation m_j to a drug d_k is associated with a weight equal to the Stanford score value $s_{m_j d_k}$ associated with that drug-mutation pair.

To further refine our representation, we created two different types of graphs for each record in the training set T :

- Type “all”: the graph G_i related to a record (x_i, y_i) includes nodes for all mutations and drugs in T .
- Type “subset”: the graph G_i related to a record (x_i, y_i) includes only the nodes for the mutations and drugs that are actually present in x_i , i.e., have attribute value 1.

Below, we will add a suffix to the model name to differentiate models trained on different types of graphs. The suffix added is “_all” or “_subset” depending on whether the model is trained on “all” or “subset” type graphs, respectively.

4.4. Datasets to simulate OoD features

The OoD features for which we want to test the prediction capabilities of the proposed model are drugs, to align with the clinical need to predict the outcome of therapies that include drugs for which there are insufficient training data. This lack of data may result from the fact that the drug is new to the market or because currently available data are incomplete or insufficient. To simulate scenarios in which a feature is not observed in the training set but is present in the test set as an OoD, we generate as many different datasets as there are OoD features on which we want to test the model. In each of these datasets, the training set consists only and exclusively of samples in which the OoD drug has value 0. This means that the training

set will contain all and only ARTs that do not involve that drug. In contrast, the test set is composed only of samples in which the OoD drug is present and valued at 1. The test set therefore will consist of all and only the ARTs that contain that drug.

4.5. Models

4.5.1. Fully Connected Neural Networks

The Fully Connected (FC) neural network takes as input a feature vector of size 5970, which is the sum of the number of mutations ($N_M = 5941$) and drugs ($N_D = 29$). The FC network architecture consists of two hidden layers with increasing sizes (64 and 256). Each hidden layer applies a linear transformation followed by a Rectified Linear Unit (ReLU) activation function. The output layer performs a linear transformation to produce the final output with a size equal to the number of output classes (2).

4.5.2. Graph Neural Networks

The GNN’s architecture consists of three hidden layers with increasing sizes (4, 8, and 16) and ReLU activation functions. The GNN layers are adopted from [53]. Each hidden layer uses the message-passing layers operation with additive attention and directed message-passing with 5 ensembles. Then a Global Max Pooling operation is performed creating a feature vector, on which the output layer performs a linear transformation to produce the final output with a size equal to the number of output classes (2).

4.5.3. MIX - Joint Fusion

The architecture of the fusion module combines the features extracted from the Graph Neural Network (GNN) and the FC networks, as illustrated

in Figure 1. For this fusion, the features from the last hidden layers of both networks are concatenated into an embedding. This embedding is then passed through a linear layer, followed by a sigmoid activation function, producing a final output vector with a size equal to the number of output classes (2). The concatenation of features allows the model to capture complementary information from both networks and make more informed predictions.

4.6. Training

The training phase involves training the GNN and the FC network independently. Then, utilizing transfer learning, the fused networks are trained in an end-to-end manner, leveraging the knowledge gained from the individual network training stages. This approach allows the fused networks to benefit from the specific features learned by each network while also capturing synergistic effects that arise from their combination. By combining the pre-trained GNN and FC networks, the fused networks can learn higher-level representations that effectively leverage the strengths of both architectures. This transfer learning strategy enhances the overall performance and enables the fused networks to make more accurate predictions compared to training them from scratch. During training, the GNN, FC, and fusion modules are trained using the Cross-Entropy Loss, which measures the difference between predicted and actual class labels. To prevent bias, the Cross-Entropy Loss is weighted based on the class distribution. The optimizer used for training is Adam with a learning rate of 0.001. The models are trained for 1000 epochs, iterating over the training dataset multiple times to optimize the network parameters and improve performance.

5. Experiments

This section explains how experiments were conducted to test the MIX model’s effectiveness in improving generalization abilities, in the case of OoD features in the test set, compared to an FC neural network.

For each drug, we trained a model without data on that drug in the training set. Then we tested the model with a test set with solely records using that drug to test the model’s ability in the case of OoD. We did not run experiments for drugs for which the procedure of dividing the data between training and test sets would have resulted in too few samples in the test set or even all data points with the same class label (all successes or all failures). In these cases, the size and quality of the test set were not adequate to obtain meaningful and reliable results.

For each model, the dataset was partitioned in a random manner into a training set, validation set, and test set with 60%, 20%, and 20% of data, respectively. The test set was reserved to evaluate the model’s ability to generalize. While randomly allocating data into training and testing subsets, particular care was exercised to ensure that various treatments related to an individual patient were grouped into the same subset. This measure was instituted to mitigate the risk that the model might inadvertently learn patterns from patients’ medical records if their treatments were scattered between the training and testing sets. Such a situation could compromise the model by skewing predictive results for future treatments given to that same patient. By consolidating treatments from the same patient into a single data subset, we aim to attenuate any undue bias and ensure that the model’s predictive capacity is grounded in unbiased generalization as opposed

to individual medical histories.

We compare the performances of the following models:

- FC: Fully connected neural network trained on tabular data presented in subsection 4.2.
- GNN_all: Graph neural network trained on samples represented in a type “all” graphs, as explained in subsection 4.3.
- GNN_subset: Graph neural network trained on samples represented in a type “subset” graphs, as explained in subsection 4.3.
- MIX_all: Fusion model that combines a GNN trained on type “all” graphs and an FC neural network trained on tabular data.
- MIX_subset: Fusion model that combines a GNN trained on type “subset” graphs and an FC neural network trained on tabular data.

The performances of GNN and MIX models are compared with those of FC by performing a paired Wilcoxon test.

6. Results

Results are shown in Table 1 and graphically reported in Figure 2. We reported the results of Accuracy (Acc), of the Receiving Operating Characteristics (ROC) area under the curve and of the precision-recall (PR) area under the curve in percentages. The choice to report these metrics is due to the fact that test sets with an OoD feature can be unbalanced by presenting more successes than failures. The rows represent the model type and the OoD column indicates which is the OoD drug in the test set.

In the case of a test set with an OoD feature, the MIX model performs best in 11 out of 15 in the ROC score and in 9 out of 15 for the PR score. The FC is better than the other models in only 1 case when we look at the ROC score and in 3 when we look at the PR. Furthermore, a statistically significant difference exists between the MIX model and the FC model in 9 out of 15 cases. This shows that the proposed model improves generalization ability compared with a FC.

Moreover, the MIX model we propose outperforms the other models when there are no OoD features in the test set with a gap in performances noticeably larger and a statistically significant difference with respect to the FC. This might suggest that the MIX models are leveraging information from both FC and GNN architectures more effectively when there is no OoD data to contend with.

Model	OoD	Acc	ROC	PR
FC	ATV	56.7	66.2	62.7
GNN_all	ATV	61.5*	64.6	59.9
GNN_subset	ATV	62.1*	64.2	60.3
MIX_all	ATV	<u>61.9</u> *	66.8	64.4
MIX_subset	ATV	61.8*	<u>66.7</u>	<u>64.3</u>
FC	DRV	58.8	59.7	<u>46.5</u>
GNN_all	DRV	60.4★	60.2	44.5
GNN_subset	DRV	63.7*	<u>60.5</u>	44.8
MIX_all	DRV	64.8*	61.0	46.6
MIX_subset	DRV	<u>64.5</u> *	61.0	46.6
FC	DTG	75.1	46.4	15.0
GNN_all	DTG	<u>75.8</u>	48.3	15.2
GNN_subset	DTG	82.7*	51.5	16.2

Table 1

Model	OoD	Acc	ROC	PR
MIX_all	DTG	72.0	<u>49.0</u>	<u>16.0</u>
MIX_subset	DTG	72.0	<u>49.0</u>	<u>16.0</u>
FC	EFV	64.5	<u>67.7</u>	<u>61.3</u>
GNN_all	EFV	62.7	65.4	60.1
GNN_subset	EFV	62.7	65.9	60.8
MIX_all	EFV	<u>64.8</u>	69.2	65.0
MIX_subset	EFV	65.0	69.2	65.0
FC	ETR	60.8	60.8	<u>49.6</u>
GNN_all	ETR	<u>61.7</u>	59.3	45.0
GNN_subset	ETR	58.7	56.7	43.8
MIX_all	ETR	62.4	<u>60.6</u>	47.4
MIX_subset	ETR	59.6	59.9	49.8
FC	EVG	74.4	56.0	18.3
GNN_all	EVG	83.2*	56.4	18.6
GNN_subset	EVG	53.6	56.6	19.1
MIX_all	EVG	72.1	<u>57.3</u>	<u>20.7</u>
MIX_subset	EVG	<u>74.9</u>	58.0	21.9
FC	FPV	64.4	<u>64.5</u>	75.1
GNN_all	FPV	64.1	63.0	<u>75.7</u>
GNN_subset	FPV	64.1	63.2	75.5
MIX_all	FPV	69.0*	67.6	77.2
MIX_subset	FPV	<u>68.9*</u>	67.6	77.2
FC	IDV	67.7	62.7	<u>77.9</u>
GNN_all	IDV	70.2*	64.5	77.7
GNN_subset	IDV	70.4*	64.5	78.3
MIX_all	IDV	71.1*	<u>63.9</u>	76.9
MIX_subset	IDV	<u>70.9</u> *	63.7	76.6
FC	LPV	62.8	66.5	<u>73.4</u>
GNN_all	LPV	61.8	64.5	72.0
GNN_subset	LPV	<u>63.2</u>	64.0	71.5
MIX_all	LPV	65.2*	67.4	73.8

Table 1

Model	OoD	Acc	ROC	PR
MIX_subset	LPV	65.2*	<u>67.3</u>	73.8
FC	NFV	<u>65.3</u>	62.5	74.0
GNN_all	NFV	63.4	61.4	73.0
GNN_subset	NFV	63.5	<u>63.6</u>	<u>74.7</u>
MIX_all	NFV	67.2*	67.0	77.9
MIX_subset	NFV	67.2*	67.0	77.9
FC	NVP	63.8	73.2	73.0
GNN_all	NVP	60.6	69.0	71.3
GNN_subset	NVP	56.3	69.1	71.0
MIX_all	NVP	<u>69.9*</u>	<u>73.8</u>	72.6
MIX_subset	NVP	70.4*	74.1	<u>72.8</u>
FC	RAL	61.6	56.9	39.2
GNN_all	RAL	49.8	57.6	38.7
GNN_subset	RAL	54.1	55.7	36.7
MIX_all	RAL	54.1	60.5	43.4
MIX_subset	RAL	<u>61.1</u>	<u>60.0</u>	<u>41.1</u>
FC	RPV	54.9	57.5	15.8
GNN_all*	RPV	83.5*	61.6	14.2
GNN_subset	RPV	<u>82.5*</u>	<u>59.2</u>	14.2
MIX_all	RPV	81.3*	56.9	15.8
MIX_subset	RPV	81.0*	56.9	<u>15.6</u>
FC	SQV	67.7	<u>60.5</u>	77.8
GNN_all	SQV	65.6	60.2	75.4
GNN_subset	SQV	<u>68.8</u>	59.8	75.7
MIX_all	SQV	69.7*	61.2	<u>76.6</u>
MIX_subset	SQV	69.7*	61.2	<u>76.6</u>
FC	TPV	75.4	59.1	79.7
GNN_all	TPV	75.7	52.1	<u>79.2</u>
GNN_subset	TPV	<u>75.5</u>	57.3	78.5
MIX_all	TPV	73.0	59.3	78.8

Table 1

Model	OoD	Acc	ROC	PR
MIX_subset	TPV	73.0	<u>59.2</u>	78.8
FC	-	71.4	78.8	72.9
GNN_all	-	68.1	72.5	65.3
GNN_subset	-	66.3	68.2	60.3
MIX_all	-	<u>76.1*</u>	<u>82.9</u>	<u>77.7</u>
MIX_subset	-	79.9*	85.8	80.4

Table 1: Models’ performances (%) on the test set. The OoD column indicates which feature is out of distribution in the test set. - indicates that there are no OoD features in the test set. The best and second-best results are in bold and underlined, respectively.

* the Wilcoxon test is significant at level 0.01, * at level 0.05

If we look at the ROC score results more in detail, we see that the only case in which FC is better than the other models it is when the OoD feature is ETR. In this case, the differences in performance between the models are not significant. This is indicative of the fact that knowledge derived from Stanford scores in this case does not help in better prediction. ETR has been the most elusive drug in terms of prediction of in-vivo effectiveness based on HIV genotype. There are three main reasons for this. First, contrary to most other drugs, ETR susceptibility is impacted by many mutations, amplifying mutation interaction effects which are difficult to examine both in-vitro and in-vivo [54, 55]. Indeed, the interpretation of susceptibility to ETR has been changed several times and alternative scores have concomitantly existed for a long time [56]. Second, due to substantial toxicity and inconvenience of dosing (twice daily instead of once daily), ETR has been used sparingly, generating few data for training genotype interpretation systems. Genotype interpretation has remained based on the original DUET trials where ETR

was combined with the highly potent DRV, hence the effects of the individual drug were largely confounded by the accompanying drug [54]. Third, drug toxicity and inconvenience of dosing per se increased the risk of treatment failure as a result of poor tolerability and low adherence to therapy rather than of true virological non-efficacy.

Looking at the PR score more in detail, we see that FC is better than the other models only when the OoD feature is TPV, SQV or NVP.

Considerations similar to the ones made for ETR certainly apply to TPV, the most potent protease inhibitor with very high genetic barrier, a highly complex resistance mutation profile and perhaps the highest toxicity ever experienced with an antiretroviral drug [57]. Indeed, TPV had very limited use in the clinic, again compromising the development of an accurate genotypic interpretation score.

Regarding SQV, particularly in the first years of use without any pharmacokinetic enhancer, suffered from very low bioavailability limiting its in-vivo effectiveness [58]. This could cause algorithms that rely on Stanford scores to be less reliable for predicting the success of SQV-containing therapies, especially in the years 1996-2001. The model therefore could predict false successes and lower the performance of PR scores.

For NVP, the FC is the model that performs best but the difference with the other models is minimal. As a resistance profile, unlike ETR and TPV, it is simple. It is worth noting that NVP is part of older therapies that generally worked less given even the other drugs combined with NVP, and thus NPV therapies could have failed more than predicted through rule-based GIS such as those using Stanford scores [59]. Consequently, even the MIX model is

helped little by the knowledge derived from Stanford scores in predicting failures.

7. Conclusions

The primary goal of this study was to predict the outcome of antiretroviral therapies for HIV-1, especially in scenarios with OoD drugs. ML models are increasingly used to guide treatment choices due to growing genotypic and clinical data. However, these models have limitations when predicting outcomes for treatments containing drugs not in their training set. This is usually because the drug is either rarely used or newly launched, making relevant data scarce. Rule-based systems also struggle with new drugs, as their susceptibility scores often rely on limited clinical experience. To face this issue, we introduced and evaluated a novel model, denoted as MIX model, a joint fusion model of a GNN and a FC neural network. Thanks to the use of graph structures, we incorporated the knowledge derived from the Stanford score in the data. These scores derive from drug-resistance mutation tables created and continually updated by experts to be used in rule-based GIS and take decisions on new HIV treatments to prescribe to PLWHIV. Our results demonstrated the superiority of our MIX model in handling OoD cases, outperforming the standalone FC model in the majority of the scenarios. Moreover, the MIX model shows superior performance compared to other models when the test set is devoid of OoD drugs. The performance gap is not only remarkable but also statistically significant compared to the FC model. This might indicate that the MIX model is more adept at synthesizing information from the FC and GNN frameworks, particularly when

no OoD data are present.

Our research underscores the value of integrating multiple data representations and neural network architectures. It establishes a foundation for improved generalizability, especially in contexts where there's limited data availability or novel data challenges. In summary, by focusing on fortifying model robustness against OoD scenarios, we pave the way for advancements that transcend traditional OoD detection methodologies, fostering a new paradigm in the field of HIV prediction and medical ML.

In future studies, we will explore further the treatment of drugs that act on pairs of mutations. As a matter of fact, there are Stanford scores that associate a drug with a pair of mutations that were not used in this study. Instead of traditional graphs that represent binary relationships, a hyper-graph can be leveraged. Hyper-graphs allow us to model higher-order relationships, thus providing a richer representation when considering drugs that interact with pairs or even sets of mutations. In the future, we will incorporate mutations detected in GRTs older than the one at baseline. Building on a prior study [60], there exists potential in using all older mutations to improve the generalization of the prediction models. This could allow the model to recognize more nuanced patterns and trends in the data. Furthermore, an interesting approach would be to consider the time frame from mutation registration when using the data. Drawing inspiration from previous research, incorporating the temporal dimension could be useful in understanding the evolutionary aspects of HIV mutations and their impact on drug resistance over time.

Competing interests

No competing interest is declared.

Author contributions statement

Giulia Di Teodoro: Conceptualization, Methodology, Software, Formal analysis of data, Investigation, Writing original draft, Review and Editing. **Federico Siciliano:** Conceptualization, Methodology, Software, Project administration, Investigation, Writing original draft, Review and Editing. **Valerio Guarrasi:** Conceptualization, Methodology, Software, Investigation, Writing original draft, Review and Editing. **Anne-Mieke Vendamme:** Data Curation and Revision of the final manuscript. **Valeria Ghisetti:** Data Curation and Revision of the final manuscript. **Anders Sönnnerborg:** Data Curation and Revision of the final manuscript. **Maurizio Zazzi:** Data Curation, Validation and interpretation of results, and Revision of the final manuscript. **Fabrizio Silvestri:** Conceptualization, Supervision, and Revision of the final manuscript. **Laura Palagi:** Conceptualization, Supervision, and Revision of the final manuscript.

Acknowledgments

The authors would like to thank the EuResist Network working group for their valuable work for the EIDB. This work was partially supported by projects FAIR (PE0000013) and SERICS (PE0000014) under the MUR National Recovery and Resilience Plan funded by the European Union - NextGenerationEU. Supported also by the ERC Advanced Grant 788893

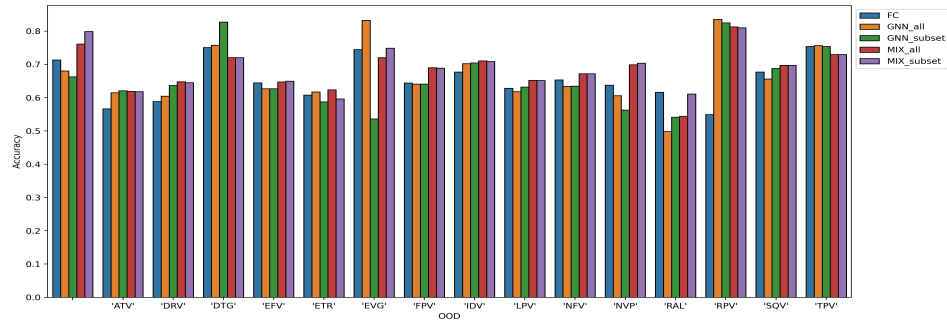
AMDROMA, EC H2020RIA project “SoBigData++” (871042), PNRR MUR project IR0000013-SoBigData.it.

Data availability statement

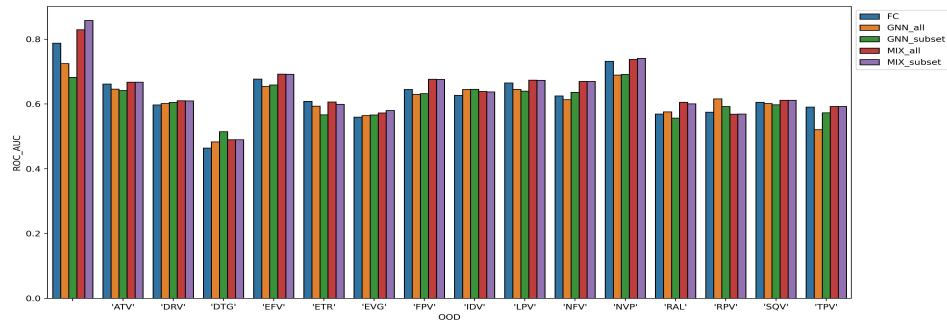
Restrictions apply to the availability of these data. Data were obtained from the EuResist Network and are available for request through a study application form at <https://www.euresist.org/become-a-partner> with the permission of the EuResist Network.

Ethic statement

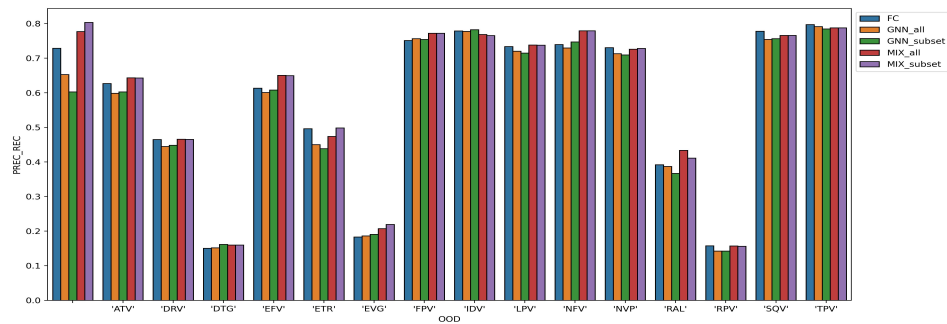
Ethical approval was granted in the host countries of the respective original databases contributing data to EIDB.



(a)



(b)



(c)

Figure 2: Panel (a) and Panel (b) and Panel (c) represent the models' test performance in Accuracy, ROC AUC score and PREC-REC AUC score, respectively. The histograms are divided per OoD features.

References

- [1] W. H. Organization, World health statistics 2023: monitoring health for the SDGs, sustainable development goals, World Health Organization, 2023.
- [2] HHS Panel on Antiretroviral Guidelines for Adults, Adolescents—A Working Group of the Office of AIDS Research Advisory Council (OARAC), Guidelines for the use of antiretroviral agents in adults and adolescents with HIVS, US Department of Health and Human Services, 2023.
- [3] L. Ryom, R. De Miguel, A. G. Cotter, D. Podlekareva, C. Beguelin, H. Waalewijn, J. R. Arribas, P. W. G. Mallon, C. Marzolini, O. Kirk, A. Bamford, A. Rauch, J. M. Molina, J. D. Kowalska, G. Guaraldi, A. Winston, C. Boesecke, P. Cinque, S. Welch, S. Collins, G. M. N. Behrens, the EACS Governing Board, Major revision version 11.0 of the european AIDS clinical society guidelines 2021, *HIV Med.* 23 (2022) 849–858.
- [4] A. M. Wensing, V. Calvez, F. Ceccherini-Silberstein, C. Charpentier, H. F. Günthard, R. Paredes, R. W. Shafer, D. D. Richman, 2022 update of the drug resistance mutations in HIV-1, *Top. Antivir. Med.* 30 (2022) 559–574.
- [5] J. A. Anderson, H. Jiang, X. Ding, L. Petch, T. Journigan, S. A. Fiscus, R. Haubrich, D. Katzenstein, R. Swanstrom, R. M. Gulick, AIDS Clinical Trials Group Study 359 Protocol Team, Genotypic suscepti-

- bility scores and HIV type 1 RNA responses in treatment-experienced subjects with HIV type 1 infection, *AIDS Res. Hum. Retroviruses* 24 (2008) 685–694.
- [6] D. Frentz, C. A. B. Boucher, M. Assel, A. De Luca, M. Fabbiani, F. Incardona, P. Libin, N. Manca, V. Müller, B. Ó. Nualláin, R. Paredes, M. Prosperi, E. Quiros-Roldan, L. Ruiz, P. M. A. Sloom, C. Torti, A.-M. Vandamme, K. Van Laethem, M. Zazzi, D. A. M. C. van de Vijver, Comparison of HIV-1 genotypic resistance test interpretation systems in predicting virological outcomes over time, *PLoS One* 5 (2010) e11505.
- [7] N. Beerenwinkel, M. Däumer, M. Oette, K. Korn, D. Hoffmann, R. Kaiser, T. Lengauer, J. Selbig, H. Walter, Geno2pheno: Estimating phenotypic drug resistance from HIV-1 genotypes, *Nucleic Acids Res.* 31 (2003) 3850–3855.
- [8] T. Lengauer, T. Sing, Bioinformatics-assisted anti-HIV therapy, *Nat. Rev. Microbiol.* 4 (2006) 790–797.
- [9] A. Pironti, N. Pfeifer, H. Walter, B.-E. O. Jensen, M. Zazzi, P. Gomes, R. Kaiser, T. Lengauer, Using drug exposure for predicting drug resistance - a data-driven genotypic interpretation tool, *PLoS One* 12 (2017) e0174992.
- [10] F. Scarselli, M. Gori, A. C. Tsoi, M. Hagenbuchner, G. Monfardini, The graph neural network model, *IEEE Trans. Neural Netw.* 20 (2009) 61–80.

- [11] A. M. Wensing, V. Calvez, F. Ceccherini-Silberstein, C. Charpentier, H. F. Günthard, R. Paredes, R. W. Shafer, D. D. Richman, 2022 update of the drug resistance mutations in HIV-1, *Top. Antivir. Med.* 30 (2022) 559–574.
- [12] M. W. Tang, R. W. Shafer, HIV-1 antiretroviral resistance: scientific principles and clinical applications, *Drugs* 72 (2012) e1–25.
- [13] M. W. Tang, T. F. Liu, R. W. Shafer, The HIVdb system for HIV-1 genotypic resistance interpretation, *Intervirology* 55 (2012) 98–101.
- [14] M. Obermeier, A. Pironti, T. Berg, P. Braun, M. Däumer, J. Eberle, R. Ehret, R. Kaiser, N. Kleinkauf, K. Korn, C. Kücherer, H. Müller, C. Noah, M. Stürmer, A. Thielen, E. Wolf, H. Walter, HIV-GRADE: a publicly available, rules-based drug resistance interpretation algorithm integrating bioinformatic knowledge, *Intervirology* 55 (2012) 102–107.
- [15] R. Paredes, P. L. Tzou, G. van Zyl, G. Barrow, R. Camacho, S. Carmona, P. M. Grant, R. K. Gupta, R. L. Hamers, P. R. Harrigan, M. R. Jordan, R. Kantor, D. A. Katzenstein, D. R. Kuritzkes, F. Maldarelli, D. Otelea, C. L. Wallis, J. M. Schapiro, R. W. Shafer, Collaborative update of a rule-based expert system for HIV-1 genotypic resistance test interpretation, *PLoS One* 12 (2017) e0181357.
- [16] C. J. Davidson, E. Zeringer, K. J. Champion, M.-P. Gauthier, F. Wang, J. Boonyaratanakornkit, J. R. Jones, E. Schreiber, Improving the limit of detection for sanger sequencing: a comparison of methodologies for KRAS variant detection, *Biotechniques* 53 (2012) 182–188.

- [17] A. C. Tsiatis, A. Norris-Kirby, R. G. Rich, M. J. Hafez, C. D. Gocke, J. R. Eshleman, K. M. Murphy, Comparison of sanger sequencing, pyrosequencing, and melting curve analysis for the detection of KRAS mutations: diagnostic and clinical implications, *J. Mol. Diagn.* 12 (2010) 425–432.
- [18] A. Cozzi-Lepri, M. Noguera-Julian, F. Di Giallonardo, R. Schuurman, M. Däumer, S. Aitken, F. Ceccherini-Silberstein, A. D’Arminio Monforte, A. M. Geretti, C. L. Booth, R. Kaiser, C. Michalik, K. Jansen, B. Masquelier, P. Bellecave, R. D. Kouyos, E. Castro, H. Furrer, A. Schultze, H. F. Günthard, F. Brun-Vezinet, R. Paredes, K. J. Metzner, CHAIN Minority HIV-1 Variants Working Group, Low-frequency drug-resistant HIV-1 and risk of virological failure to first-line NNRTI-based ART: a multicohort european case-control study using centralized ultrasensitive 454 pyrosequencing, *J. Antimicrob. Chemother.* 70 (2015) 930–940.
- [19] B. Vrancken, N. S. Trovão, G. Baele, E. van Wijngaerden, A.-M. Vandamme, K. van Laethem, P. Lemey, Quantifying next generation sequencing sample pre-processing bias in HIV-1 complete genome sequencing, *Viruses* 8 (2016) 12.
- [20] E. J. Fox, K. S. Reid-Bayliss, M. J. Emond, L. A. Loeb, Accuracy of next generation sequencing platforms, *Next Gener. Seq. Appl.* 1 (2014).
- [21] H. Vermeiren, E. Van Craenenbroeck, P. Alen, L. Bacheler, G. Picchio, P. Lecocq, Virco Clinical Response Collaborative Team, Prediction of

- HIV-1 drug susceptibility phenotype from the viral genotype using linear regression modeling, *J. Virol. Methods* 145 (2007) 47–55.
- [22] N. Beerenwinkel, M. Däumer, M. Oette, K. Korn, D. Hoffmann, R. Kaiser, T. Lengauer, J. Selbig, H. Walter, Geno2pheno: Estimating phenotypic drug resistance from HIV-1 genotypes, *Nucleic Acids Res.* 31 (2003) 3850–3855.
- [23] B. Winters, J. Montaner, P. R. Harrigan, B. Gazzard, A. Pozniak, M. D. Miller, S. Emery, F. van Leth, P. Robinson, J. D. Baxter, M. Perez-Elias, D. Castor, S. Hammer, A. Rinehart, H. Vermeiren, E. Van Craenenbroeck, L. Bachelier, Determination of clinically relevant cutoffs for HIV-1 phenotypic resistance estimates through a combined analysis of clinical trial and cohort data, *J. Acquir. Immune Defic. Syndr.* 48 (2008) 26–34.
- [24] A. Altmann, M. Däumer, N. Beerenwinkel, Y. Peres, E. Schülter, J. Büch, S.-Y. Rhee, A. Sönnernborg, W. J. Fessel, R. W. Shafer, M. Zazzi, R. Kaiser, T. Lengauer, Predicting the response to combination antiretroviral therapy: retrospective validation of geno2pheno-THEO on a large clinical database, *J. Infect. Dis.* 199 (2009) 999–1006.
- [25] A. Pironti, H. Walter, N. Pfeifer, E. Knops, N. Lübke, J. Büch, S. Di Giambenedetto, R. Kaiser, T. Lengauer, EuResist Network Study Group, Determination of phenotypic resistance cutoffs from routine clinical data, *J. Acquir. Immune Defic. Syndr.* 74 (2017) e129–e137.

- [26] T. Lengauer, T. Sing, Bioinformatics-assisted anti-HIV therapy, *Nat. Rev. Microbiol.* 4 (2006) 790–797.
- [27] A. Pironti, N. Pfeifer, H. Walter, B.-E. O. Jensen, M. Zazzi, P. Gomes, R. Kaiser, T. Lengauer, Using drug exposure for predicting drug resistance – a data-driven genotypic interpretation tool, *PLOS ONE* 12 (2017) 1–27. URL: <https://doi.org/10.1371/journal.pone.0174992>. doi:10.1371/journal.pone.0174992.
- [28] M. Riemenschneider, T. Hummel, D. Heider, Shiva - a web application for drug resistance and tropism testing in hiv, *BMC Bioinformatics* 17 (2016).
- [29] B. Larder, D. Wang, A. Revell, J. Montaner, R. Harrigan, F. De Wolf, J. Lange, S. Wegner, L. Ruiz, M. J. Pérez-Elías, S. Emery, J. Gatell, A. D. Monforte, C. Torti, M. Zazzi, C. Lane, The development of artificial neural networks to predict virological response to combination HIV therapy, *Antivir. Ther.* 12 (2007) 15–24.
- [30] D. Hendrycks, K. Gimpel, A baseline for detecting misclassified and out-of-distribution examples in neural networks, *arXiv preprint arXiv:1610.02136* (2016).
- [31] S. Liang, Y. Li, R. Srikant, Enhancing the reliability of out-of-distribution image detection in neural networks, *arXiv preprint arXiv:1706.02690* (2017).
- [32] B. Lakshminarayanan, A. Pritzel, C. Blundell, Simple and scalable

- predictive uncertainty estimation using deep ensembles, *Advances in neural information processing systems* 30 (2017).
- [33] T. Cao, C.-W. Huang, D. Y.-T. Hui, J. P. Cohen, A benchmark of medical out of distribution detection, *arXiv preprint arXiv:2007.04250* (2020).
- [34] D. Zimmerer, P. M. Full, F. Isensee, P. Jäger, T. Adler, J. Petersen, G. Köhler, T. Ross, A. Reinke, A. Kascenas, et al., Mood 2020: A public benchmark for out-of-distribution detection and localization on medical images, *IEEE Transactions on Medical Imaging* 41 (2022) 2728–2738.
- [35] K. Zadorozhny, P. Thorat, P. Elbers, G. Cinà, Out-of-distribution detection for medical applications: Guidelines for practical evaluation, in: *Multimodal AI in healthcare: A paradigm shift in health intelligence*, Springer, 2022, pp. 137–153.
- [36] Z. Wu, S. Pan, F. Chen, G. Long, C. Zhang, S. Y. Philip, A comprehensive survey on graph neural networks, *IEEE transactions on neural networks and learning systems* 32 (2020) 4–24.
- [37] S. Zhang, H. Tong, J. Xu, R. Maciejewski, Graph convolutional networks: a comprehensive review, *Computational Social Networks* 6 (2019) 1–23.
- [38] X.-M. Zhang, L. Liang, L. Liu, M.-J. Tang, Graph neural networks and their current applications in bioinformatics, *Frontiers in genetics* 12 (2021) 690049.

- [39] M. Sun, S. Zhao, C. Gilvary, O. Elemento, J. Zhou, F. Wang, Graph convolutional networks for computational drug development and discovery, *Briefings in bioinformatics* 21 (2020) 919–935.
- [40] K. Jha, S. Saha, H. Singh, Prediction of protein–protein interaction using graph neural networks, *Scientific Reports* 12 (2022) 8360.
- [41] J. Wang, A. Ma, Q. Ma, D. Xu, T. Joshi, Inductive inference of gene regulatory network using supervised and semi-supervised graph neural networks, *Computational and structural biotechnology journal* 18 (2020) 3335–3343.
- [42] H. Cui, W. Dai, Y. Zhu, X. Kan, A. A. C. Gu, J. Lukemire, L. Zhan, L. He, Y. Guo, C. Yang, Braingb: A benchmark for brain network analysis with graph neural networks, *IEEE transactions on medical imaging* 42 (2022) 493–506.
- [43] Z. Liu, X. Li, H. Peng, L. He, S. Y. Philip, Heterogeneous similarity graph neural network on electronic health records, in: *2020 IEEE International Conference on Big Data (Big Data)*, IEEE, 2020, pp. 1196–1205.
- [44] A. Bessadok, M. A. Mahjoub, I. Rekik, Graph neural networks in network neuroscience, *IEEE Transactions on Pattern Analysis and Machine Intelligence* 45 (2022) 5833–5848.
- [45] D. Jiang, Z. Wu, C.-Y. Hsieh, G. Chen, B. Liao, Z. Wang, C. Shen, D. Cao, J. Wu, T. Hou, Could graph neural networks learn better molecular representation for drug discovery? a comparison study of

- descriptor-based and graph-based models, *Journal of cheminformatics* 13 (2021) 1–23.
- [46] G. Bouritsas, F. Frasca, S. Zafeiriou, M. M. Bronstein, Improving graph neural network expressivity via subgraph isomorphism counting, *IEEE Transactions on Pattern Analysis and Machine Intelligence* 45 (2022) 657–668.
- [47] B. Das, M. Kutsal, R. Das, Effective prediction of drug – target interaction on hiv using deep graph neural networks, *Chemometrics and Intelligent Laboratory Systems* 230 (2022) 104676. URL: <https://www.sciencedirect.com/science/article/pii/S0169743922001873>. doi:<https://doi.org/10.1016/j.chemolab.2022.104676>.
- [48] J. Zhang, Y. Du, P. Zhou, J. Ding, S. Xia, Q. Wang, F. Chen, M. Zhou, X. Zhang, W. Wang, H. Wu, L. Lu, S. Zhang, Predicting unseen antibodies’ neutralizability via adaptive graph neural networks, *Nat. Mach. Intell.* 4 (2022) 964–976.
- [49] Y. Wang, Y. Li, X. Chen, L. Zhao, Hiv-1/hbv coinfection accurate multitarget prediction using a graph neural network-based ensemble predicting model, *International Journal of Molecular Sciences* 24 (2023). URL: <https://www.mdpi.com/1422-0067/24/8/7139>. doi:10.3390/ijms24087139.
- [50] B. Rossetti, F. Incardona, G. Di Teodoro, C. Mommo, F. Saladini, R. Kaiser, A. Sönnernborg, T. Lengauer, M. Zazzi, Cohort profile: A european multidisciplinary network for the fight against hiv drug re-

- sistance (euresist network), *Tropical Medicine and Infectious Disease* 8 (2023). URL: <https://www.mdpi.com/2414-6366/8/5/243>. doi:10.3390/tropicalmed8050243.
- [51] M. Zazzi, R. Kaiser, A. Sönnnerborg, D. Struck, A. Altmann, M. Prospero, M. Rosen-Zvi, A. Petroczi, Y. Peres, E. Schülter, C. A. Boucher, F. Brun-Vezinet, P. R. Harrigan, L. Morris, M. Obermeier, C.-F. Perno, P. Phanuphak, D. Pillay, R. W. Shafer, A.-M. Vandamme, K. van Laethem, A. M. J. Wensing, T. Lengauer, F. Incardona, Prediction of response to antiretroviral therapy by human experts and by the Euresist data-driven expert system (the EVE study), *HIV Med.* 12 (2011) 211–218.
- [52] R. W. Shafer, S.-Y. Rhee, D. Pillay, V. Miller, P. Sandstrom, J. M. Schapiro, D. R. Kuritzkes, D. Bennett, HIV-1 protease and reverse transcriptase mutations for drug resistance surveillance, *AIDS* 21 (2007) 215–223.
- [53] J. You, R. Ying, J. Leskovec, Design space for graph neural networks, in: *Proceedings of the 34th International Conference on Neural Information Processing Systems, NIPS’20*, Curran Associates Inc., Red Hook, NY, USA, 2020.
- [54] J. Vingerhoets, L. Tambuyzer, H. Azijn, A. Hoogstoel, S. Nijs, M. Peeters, M.-P. de Béthune, G. De Smedt, B. Woodfall, G. Picchio, Resistance profile of etravirine: combined analysis of baseline genotypic and phenotypic data from the randomized, controlled phase III clinical studies, *AIDS* 24 (2010) 503–514.

- [55] R. M. Kagan, P. Sista, T. Pattery, L. Bacheler, D. A. Schwab, Additional HIV-1 mutation patterns associated with reduced phenotypic susceptibility to etravirine in clinical samples, *AIDS* 23 (2009) 1602–1605.
- [56] J. Vingerhoets, S. Nijs, L. Tambuyzer, A. Hoogstoel, D. Anderson, G. Picchio, Similar predictions of etravirine sensitivity regardless of genotypic testing method used: comparison of available scoring systems, *Antivir. Ther.* 17 (2012) 1571–1579.
- [57] B. Vergani, S. Rusconi, Tipranavir in the protease inhibitors arena, *Drugs R. D.* 11 (2011) 291–293.
- [58] A. C. Collier, R. W. Coombs, D. A. Schoenfeld, R. L. Bassett, J. Timponi, A. Baruch, M. Jones, K. Facey, C. Whitacre, V. J. McAuliffe, H. M. Friedman, T. C. Merigan, R. C. Reichman, C. Hooper, L. Corey, Treatment of human immunodeficiency virus infection with saquinavir, zidovudine, and zalcitabine. AIDS clinical trials group, *N. Engl. J. Med.* 334 (1996) 1011–1017.
- [59] S. Sungkanuparph, W. Manosuthi, S. Kiertiburanakul, B. Piyavong, N. Chumpathat, W. Chantratita, Options for a second-line antiretroviral regimen for HIV type 1-infected patients whose initial regimen of a fixed-dose combination of stavudine, lamivudine, and nevirapine fails, *Clin. Infect. Dis.* 44 (2007) 447–452.
- [60] G. Di Teodoro, M. Pirkl, F. Incardona, I. Vicenti, A. Sönnnerborg, R. Kaiser, L. Palagi, M. Zazzi, T. Lengauer, Incorporating temporal

dynamics of mutations to enhance the prediction capability of antiretroviral therapy's outcome for HIV-1, 2023. [arXiv:2311.04846](https://arxiv.org/abs/2311.04846).